ACOUSTICS 2012

A multiple-scales perturbation approach to mode coupling in periodic plates

O. Asfar[a], M. Hawwa[b], M. Bavencoffe[c], B. Morvan[d] and J.-L. Izbicki[e]

[a]Jordan University of Science & Technology, Box 3030, 22110 Irbid, Jordan
[b]King Fahd University of Petroleum & Minerals, Department of Mechanical Engineering, 31261 Dhahran, Saudi Arabia
[c]Laboratoire Imagerie et Cerveau, rue de la chocolaterie BP 3410, 41034 Blois, France
[d]Laboratoire Ondes et Milieux Complexes, FRE-3102 CNRS, Place Robert Schuman, 76610 Le Havre, France
[e]LOMC, CNRS UMR 6294, Université Le Havre, 25, rue Philippe Lebon, 76600 Le Havre, France
a_s_f_a_r@yahoo.com

In this paper, guided ultrasonic wave propagation is analyzed in an elastic plate with sinusoidal surface corrugations. The corrugated area acts as a finite length grating which corresponds to a 1D phononic crystal (PC). The multiple-scales perturbation technique is used to derive coupled-mode equations describing the amplitudes of interacting modes. These equations are solved exactly for the two-point boundary-value problem of the PC. The study involved the coupling of the incident symmetric Lamb wave S_0 to the reflected antisymmetric Lamb wave A_0. The influence of the depth of corrugation and length of the PC is studied. Theoretical results are compared with experimental measurements.

1 Introduction

Nondestructive testing of surfaces and interfaces depends on the reflection of ultrasound from defects or voids assuming the surfaces to be smooth. When surface roughness is present, additional reflection becomes superimposed upon the signal and thus influences the accuracy of measurement. A special case of interest is the reflection of Lamb waves as a result of mode conversion in periodic gratings. For more than a decade, this problem has attracted the attention of several research groups in trying to come up with an analytical model to accurately and efficiently describe the phenomenon of mode conversion from the symmetric S_0 wave to the antisymmetric A_0 wave. Techniques of treating the problem of wave scattering from rough surfaces, whether in acoustics or electromagnetics, can be grouped into two main categories: analytical methods (using integral equations or perturbation methods) and numerical simulation methods. Owing to the vast amount of literature on the subject, we only cite representative publications.

The integral equation approach was the basis of a number of investigations. Lobkis and Chimenti [1,2] used the Kirchhoff phase-screen approximation to calculate the effect of random rough surfaces on the reflected signal and compared theoretical results with experiment. Their model had the principal shortcoming of the absence of its dependence on the roughness correlation length. El-Bahrawy [3] used a modal approach and derived the dispersion relation that predicted the stopbands and passbands for symmetric Lamb waves in corrugated plates. Banerjee and Kundu [4] used the null-field approach developed by Waterman [5] to study the stopbands and passbands of an elastic plate with sinusoidally varying thickness. Their approach is limited to finding a dispersion relation and predicted mode conversion from symmetric to antisymmetric modes. Valier-Brasier *et al*. [6] made an attempt to develop an analytical model for treating Lamb wave coupling in rough isotropic plates by using an integral formulation using Green's functions in which the solutions are obtained numerically through an iterative process.

Perturbation methods for periodic waveguides with periodic boundary corrugations were treated by Nayfeh [7] and Asfar *et al*. [8,9] by using the method of multiple scales. Only modes that are solutions of the same eigenvalue problem satisfying a single resonance condition or a number of simultaneous resonance conditions were treated in these works.

Leduc *et al.* , Morvan *et al*., and Bavencoffe *et al*. [10,11,12] used the finite element method to study the dispersion curves and mode conversion of the different Lamb modes in corrugated plates taking into account the resonance conditions of the harmonics of a triangular and a square surface profile in addition to sinusoidal corrugations. They also performed experiments and studied the evolution of the propagating modes in space-time by applying the fast Fourier transform to the measured data.

In the present paper, we develop an analytical model of mode coupling of counterpropagating symmetric and antisymmetric modes by applying the method of multiple scales [8].The coupling of counterpropagating modes leads to opening of a gap in the dispersion curves which is also known as a hybridization gap [11]. By carrying out a first-order perturbation expansion, coupled amplitude equations are derived and solved exactly for the two-point problem of a plate with sinusoidal surface roughness. In the case of general periodic corrugations, the model applies to the first harmonic of the surface corrugaion function. The accuracy of the model is compared with the results of an experiment.

2 Problem formulation

We consider Lamb wave propagation in the plate having thickness 2h shown in Fig.1. An x-y-z coordinate system is introduced with the x axis in the direction of wave propagation and it is assumed that the fields are independent of y. Coordinates are made dimensionless by normalizing with respect to h. The wavy upper surface is described by $z = 1 + \epsilon sink_w x$, where k_w is the dimensionless wall wavenumber and ϵ is the dimensionless wall corrugation amplitude. The lower surface of the plate is thus at z = - 1. Assuming a temporal dependence of the form $e^{-i\omega t}$, the governing equations for the scalar potential ϕ and vector potential ψ_y are respectively given by

$$\frac{\partial^2\phi}{\partial z^2} + \frac{\partial^2\phi}{\partial x^2} + k_l^2\phi = 0 \tag{1}$$

$$\frac{\partial^2\psi_y}{\partial z^2} + \frac{\partial^2\psi_y}{\partial x^2} + k_s^2\psi_y = 0 \tag{2}$$

Here k_l and k_s are given respectively by $k_l = \omega h\sqrt{\frac{\rho}{\lambda+2\mu}}$ and $k_s = \omega h\sqrt{\frac{\rho}{\mu}}$, where λ and μ are the Lamé constants. The displacement components in the x and z directions are respectively given by $u_x = \frac{\partial\phi}{\partial x} - \frac{\partial\psi_y}{\partial z}$ and $u_z = \frac{\partial\phi}{\partial z} + \frac{\partial\psi_y}{\partial x}$.

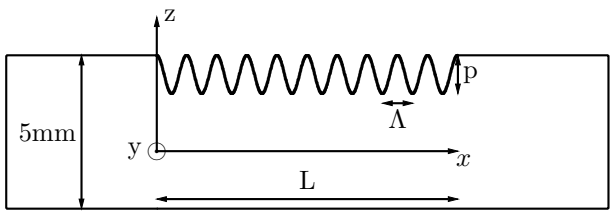

Figure 1: Corrugated plate geometry.

The boundary conditions at the wavy surface are derived from the vanishing of the traction force by finding the dot product of the stress tensor with the outward normal vector

$\mathbf{n} = \mathbf{a_z} - \epsilon k_w cos(k_w x)\mathbf{a_x}$. This leads to the following two conditions

$$-\epsilon k_w cos(k_w x)\sigma_{xx} + \sigma_{xz} = 0 \quad (3)$$

$$-\epsilon k_w cos(k_w x)\sigma_{xz} + \sigma_{zz} = 0 \quad (4)$$

where the stress components σ_{xx}, σ_{xz}, and σ_{zz} are given by

$$\sigma_{xx} = (\lambda + 2\mu)\frac{\partial^2\phi}{\partial x^2} + \lambda\frac{\partial^2\phi}{\partial z^2} - 2\mu\frac{\partial^2\psi_y}{\partial x\partial z} \quad (5)$$

$$\sigma_{xz} = \mu\left[\frac{\partial^2\psi_y}{\partial x^2} - \frac{\partial^2\psi_y}{\partial z^2} + 2\frac{\partial^2\phi}{\partial x\partial z}\right] \quad (6)$$

$$\sigma_{zz} = (\lambda + 2\mu)\frac{\partial^2\phi}{\partial z^2} + \lambda\frac{\partial^2\phi}{\partial x^2} + 2\mu\frac{\partial^2\psi_y}{\partial x\partial z} \quad (7)$$

The same boundary conditions with $\epsilon = 0$ apply at $z = -1$.

3 Multiple scales analysis

Using the method of multiple scales [8], we seek first-order asymptotic expansions for the scalar and vector potentials in the form $\phi = \phi_0 + \epsilon\phi_1$ and $\psi_y = \psi_0 + \epsilon\psi_1$. The functions ϕ_0 and ψ_0 are solutions of the reduced homogeneous problems of the uncorrugated plate, while the functions ϕ_1 and ψ_1 are small perturbations governed by inhomogeneous equations and inhomogeneous boundary conditions. We introduce the two spatial scales: $x_0 = x$ as a short length scale measuring distances of the order of a guided wavelength, and $x_1 = \epsilon x$ as a long length scale measuring the slow amplitude and phase modulations. According to these expansions, the boundary conditions at the corrugated surface are transferred to the mean boundary at $z = +1$ by expanding in Taylor's series. For the sake of brevity, we only give here the first order equations governing the perturbations of the scalar and vector potentials. The solution of the homogeneous problem is the well-known symmetric and antisymmetric mode solutions [13]:

$$\phi_{s0} = A\, cos(\alpha_l z)\, e^{ik_{sx}x_o}, \quad \psi_{A0} = C\, sin(\alpha_s z)\, e^{ik_{sx}x_o} \quad (8)$$

for the symmetric mode S_0 where α_l and α_s, given by $\alpha_l^2 = k_l^2 - k_{sx}^2$ and $\alpha_s^2 = k_s^2 - k_{sx}^2$, are solutions of the eigenvalue equation for symmetric modes , while

$$\phi_{A0} = B\, sin(\beta_l z)\, e^{-ik_{Ax}x_o}, \quad \psi_{s0} = D\, cos(\beta_s z)\, e^{-ik_{Ax}x_o} \quad (9)$$

represent the antisymmetric mode A_0 where β_l and β_s, given by $\beta_l^2 = k_l^2 - k_{Ax}^2$ and $\beta_s^2 = k_s^2 - k_{Ax}^2$, are solutions of the eigenvalue equation for antisymmetric modes.

In order to solve the problem of mode coupling of an incident S_0 wave and a reflected A_0 wave, we take the solution of the reduced problem as a linear combination of these two modes in the form

$$\phi_0 = A(x_1)cos(\alpha_l z)e^{ik_{sx}x_o} + B(x_1)\, sin(\beta_l z)e^{-ik_{Ax}x_o} \quad (10)$$

$$\psi_0 = C(x_1)\, sin(\alpha_s z)e^{ik_{sx}x_o} + D(x_1)cos(\beta_s z)e^{-ik_{Ax}x_o} \quad (11)$$

The arbitrary functions $A(x_1), B(x_1), C(x_1)$, and $D(x_1)$ are to be determined from the solvability conditions of the first-order problem. Since the same equations apply to both the symmetric and antisymmetric modes, we only state the equations for one of them (the symmetric mode). The equations for the antisymmetric mode are then simply obtained by exchanging the subscripts s and A and replacing α by β in the equations of the symmetric mode.Thus, the governing equations to O(ϵ) become

$$\frac{\partial^2\phi_{1s}}{\partial z^2} + \alpha_l^2\phi_{1s} = -2\frac{\partial^2\phi_{0s}}{\partial x_0\partial x_1} \quad (12)$$

$$\frac{\partial^2\psi_{1A}}{\partial z^2} + \alpha_s^2\psi_{1A} = -2\frac{\partial^2\psi_{0A}}{\partial x_0\partial x_1} \quad (13)$$

In writing the boundary conditions and in the spirit of the method of multiple scales, we only keep the resonant terms (terms multiplying $sin(k_w x_0)$ and $cos(k_w x_0)$) and discard the nonresonant ones. Thus, the symmetric mode boundary conditions at the corrugated boundary near $z = +1$ reduce to

$$\mu\left(\frac{\partial^2\psi_{1A}}{\partial x_0^2} - \frac{\partial^2\psi_{1A}}{\partial z^2} + 2\frac{\partial^2\phi_{1s}}{\partial x_0\partial z}\right) = -2\mu\left(\frac{\partial^2\psi_{0A}}{\partial x_0\partial x_1} + \frac{\partial^2\phi_{0s}}{\partial x_1\partial z}\right)$$
$$-\mu\, sin(k_w x_0)\left(\frac{\partial^3\psi_{0s}}{\partial x_0^2\partial z} - \frac{\partial^3\psi_{0s}}{\partial z^3} + 2\frac{\partial^3\phi_{0A}}{\partial x_0\partial z^2}\right)$$
$$+k_w\, cos(k_w x_0)\left((\lambda + 2\mu)\frac{\partial^2\phi_{0A}}{\partial x_0^2} + \lambda\frac{\partial^2\phi_{0A}}{\partial z^2} - 2\mu\frac{\partial^2\psi_{0s}}{\partial x_0\partial z}\right) \quad (14)$$

$$(\lambda + 2\mu)\frac{\partial^2\phi_{1s}}{\partial z^2} + \lambda\frac{\partial^2\phi_{1s}}{\partial x_0^2} + 2\mu\frac{\partial^2\psi_{1A}}{\partial x_0\partial z} =$$
$$-2\lambda\frac{\partial^2\phi_{0s}}{\partial x_0\partial x_1} - 2\mu\frac{\partial^2\psi_{0A}}{\partial x_1\partial z}$$
$$-sin(k_w x_0)\left((\lambda + 2\mu)\frac{\partial^3\phi_{0A}}{\partial z^3} + \lambda\frac{\partial^3\phi_{0A}}{\partial x_0^2\partial z} + 2\mu\frac{\partial^3\psi_{0s}}{\partial x_0\partial z^2}\right) \quad (15)$$

The boundary conditions at $z = -1$ become

$$\frac{\partial^2\psi_{1A}}{\partial x_0^2} - \frac{\partial^2\psi_{1A}}{\partial z^2} + 2\frac{\partial^2\phi_{1s}}{\partial x_0\partial z} = -2\frac{\partial^2\psi_{0A}}{\partial x_0\partial x_1} - 2\frac{\partial^2\phi_{0s}}{\partial x_1\partial z} \quad (16)$$

$$(\lambda+2\mu)\frac{\partial^2\phi_{1s}}{\partial z^2} + \lambda\frac{\partial^2\phi_{1s}}{\partial x_0^2} + 2\mu\frac{\partial^2\psi_{1A}}{\partial x_0\partial z} = -2\lambda\frac{\partial^2\phi_{0s}}{\partial x_0\partial x_1} - 2\mu\frac{\partial^2\psi_{0A}}{\partial x_1\partial z} \quad (17)$$

Next, we assume solutions of the first-order problem for the potential functions in the forms $\phi_{1s} = \Gamma(z)e^{ik_{sx}x_o}$, $\psi_{1A} = \Lambda(z)e^{ik_{sx}x_o}$, $\phi_{1A} = \Omega(z)e^{-ik_{Ax}x_o}$, and $\psi_{1s} = N(z)e^{-ik_{Ax}x_o}$. This leads to the following governing equations to $O(\epsilon)$

$$\frac{d^2\Gamma}{dz^2} + \alpha_l^2\Gamma = -2ik_{sx}\frac{dA}{dx_1}cos(\alpha_l z) \quad (18)$$

$$\frac{d^2\Lambda}{dz^2} + \alpha_s^2\Lambda = 2k_{sx}\gamma_s\frac{dA}{dx_1}sin(\alpha_s z) \quad (19)$$

$$\frac{d^2\Omega}{dz^2} + \beta_l^2\Omega = 2ik_{Ax}\frac{dB}{dx_1}sin(\beta_l z) \quad (20)$$

$$\frac{d^2N}{dz^2} + \beta_s^2 N = -2k_{Ax}\gamma_A\frac{dB}{dx_1}cos(\beta_s z) \quad (21)$$

The constants γ_s and γ_A are given in the Appendix. Since the right-hand sides of the governing equations are solutions of the homogeneous problem, a solution that is uniformly valid to $O(\epsilon)$ can be found if, and only if, a solvability condition is satisfied. This condition requires that the solution of the inhomogeneous problem be orthogonal to the solution of the adjoint homogeneous problem. To find the solvability condition for each mode, we need to determine the resonant coupling terms that arise in the boundary conditions at the upper wall of the plate. We also consider the case when

the modes are not in exact resonance but in a state of near resonance. This would allow us to investigate the spectral response of the mode coupling phenomenon by introducing a detuning parameter σ of O(1) that measures the nearness to resonance. Thus we express the resonance condition coupling the symmetric and antisymmetric modes by the relation $k_{sx} - k_w = -k_{Ax} + \epsilon\sigma$ and substitute the assumed solutions of the first-order potentials into Eqs.(14-17). By equating the coefficients of $e^{ik_{sx}x_o}$ on both sides of every equation, we arrive at the following boundary conditions for the symmetric mode:

$$\mu\left((\alpha_z^2 - k_{sx}^2)\Lambda(1) + 2ik_{sx}\frac{d\Gamma}{dz}(1)\right) = -Q_{11}Be^{-i\sigma x_1} + 2\mu\left[\alpha_l sin\alpha_l + 2\gamma_s k_{sx} sin\alpha_s\right]\frac{dA}{dx_1} \quad (22)$$

$$-\left(\lambda(\alpha_l^2 + k_{sx}^2) + 2\mu\alpha_l^2\right)\Gamma(1) + 2i\mu k_{sx}\frac{d\Lambda}{dz}(1) = iQ_{12}e^{-i\sigma x_1} + 2i\mu\left[2k_{sx}cos\alpha_l - \alpha_s cos\alpha_s\right]\frac{dA}{dx_1} \quad (23)$$

$$(\alpha_s^2 - k_{sx}^2)\Lambda(-1) + 2ik_{sx}\frac{d\Gamma}{dz}(-1) = 2\left[2k_{sx}\gamma_s in\alpha_s + \alpha_l sin\alpha_l\right]\frac{dA}{dx_1} \quad (24)$$

$$-\left[(\lambda + 2\mu)\alpha_l^2 + \lambda k_{sx}^2\right]\Gamma(-1) + 2i\mu k_{sx}\frac{d\Lambda}{dz}(-1) = 2i\mu\left[2k_{sx}cos\alpha_l - \alpha_s\gamma_s cos\alpha_s\right]\frac{dA}{dx_1} \quad (25)$$

The constants Q_{11} and Q_{12} are given in the Appendix. Application of the same procedure to the antisymmetric mode leads to the following boundary conditions:

$$\mu(\beta_s^2 - k_{Ax}^2)N(1) - 2i\mu k_{Ax}\frac{d\Omega}{dz}(1) = Q_{21}Ae^{i\sigma x_1} - 2\mu\left[\beta_l cos\beta_l + 2\gamma_A k_{Ax} cos\beta_s\right]\frac{dB}{dx_1} \quad (26)$$

$$\left[(\lambda + 2\mu)\beta_l^2 + \lambda k_{Ax}^2\right]\Omega(1) + 2i\mu K_{Ax}\frac{dN}{dz}(1) = -iQ_{22}Ae^{i\sigma x_1} + 2i\mu\left[2k_{Ax}sin\beta_l - \beta_s\gamma_A sin\beta_s\right]\frac{dB}{dx_1} \quad (27)$$

$$(\beta_s^2 - k_{Ax}^2)N(-1) - 2ik_{Ax}\frac{d\Omega}{dz}(-1) = -\left[4\gamma_A k_{Ax} cos\beta_s + 2\beta_l cos\beta_l\right]\frac{dB}{dx_1} \quad (28)$$

$$\left[\lambda(\beta_l^2 + k_{Ax}^2) + 2\mu\beta_l^2\right]\Omega(-1) + 2i\mu k_{Ax}\frac{dN}{dz}(-1) = -2i\mu\left[2k_{Ax}sin\beta_l - \beta_s\gamma_A sin\beta_s\right]\frac{dB}{dx_1} \quad (29)$$

The constants Q_{21} and Q_{22} are given in the Appendix.

4 Coupled-mode equations

In order to find the solvability condition for each mode, we note that the governing differential equations Eqs.(18)-(21) are self-adjoint, and hence we multiply each governing equation by the solution of its homogeneous problem and integrate by parts from z = - 1 to z = +1. The results of this procedure for both modes are the equations

$$\alpha_l sin\alpha_l\left[\Gamma(1) + \Gamma(-1)\right] - cos\alpha_l\left[\frac{d\Gamma}{dz}(1) - \frac{d\Gamma}{dz}(-1)\right] = -ik_{sx}\left(2 + \frac{sin2\alpha_l}{\alpha_l}\right)\frac{dA}{dx_1} \quad (30)$$

$$\alpha_s cos\alpha_s\left[\Lambda(1) - \Lambda(-1)\right] - sin\alpha_s\left[\frac{d\Lambda}{dz}(1) + \frac{d\Lambda}{dz}(-1)\right] = -k_{sx}\left(2 - \frac{sin2\alpha_s}{\alpha_s}\right)\gamma_s\frac{dA}{dx_1} \quad (31)$$

$$\beta_l cos\beta_l\left[\Omega(1) - \Omega(-1)\right] - sin\beta_l\left[\frac{d\Omega}{dz}(1) + \frac{d\Omega}{dz}(-1)\right] = -ik_{Ax}\left(2 - \frac{sin2\beta_l}{\beta_l}\right)\frac{dB}{dx_1} \quad (32)$$

$$\beta_s sin\beta_s\left[N(1) + N(-1)\right] + cos\beta_s\left[\frac{dN}{dz}(1) - \frac{dN}{dz}(-1)\right] = -k_{Ax}\gamma_A\left(2 + \frac{sin2\beta_s}{beta_s}\right)\frac{dB}{dx_1} \quad (33)$$

We illustrate the process of finding the coupled-mode equation for the symmetric mode by using Eqs.(22)-(25) to eliminate the derivatives $\frac{d\Gamma}{dz}(\pm1)$ and $\frac{d\Lambda}{dz}(\pm1)$ from Eqs.(30) and (31). This leads to two inhomogeneous algebraic equations for the groups $\Gamma(1)+\Gamma(-1)$ and $\Lambda(1)-\Lambda(-1)$ as two independent variables. The determinant of coefficients of this new system of equations vanishes (being the eigenvalue equation for symmetric modes) and hence by using Cramer's rule we arrive at the coupled-mode equation for the symmetric mode S_0 as

$$\zeta_{11}\frac{dA}{dx_1} = \zeta_{12}\,B\,e^{-i\sigma x_1} \quad (34)$$

Similarly, we can use Eqs.(26)-(29) to eliminate the derivatives $\frac{d\Omega}{dz}(\pm1)$ and $\frac{dN}{dz}(\pm1)$ from Eqs.(32) and (33) to arrive by the same procedure at the coupled-mode equation for the antisymmetric mode A_0 as

$$\zeta_{22}\frac{dB}{dx_1} = \zeta_{21}\,A\,e^{i\sigma x_1} \quad (35)$$

The coefficients ζ_{ij} for i,j=1,2 are given in the Appendix. These two equations have an exact solution satisfying the two-point boundary conditions A(0)=1 and B(L)=0 , where L is the length of the grating. The solution for the amplitude of the reflected antisymmetric mode A_0 is given by

$$B(x_1) = 2i\frac{\zeta_{21}\sqrt{V}}{\zeta_{22}\Delta}cos\left[\sqrt{V}(x_1 - L)\right]e^{i\frac{\sigma}{2}(x_1+L)} \quad (36)$$

where $V = \sigma^2 - \frac{4\zeta_{12}\zeta_{21}}{\zeta_{11}\zeta_{22}}$ and Δ is given by

$$\Delta = \left[-V\,cos(\sqrt{V}\frac{L}{2}) + i\sigma\sqrt{V}\,sin(\sqrt{V}\frac{L}{2})\right] \quad (37)$$

5 Analytical results

The result for the reflected antisymmetric mode amplitude in the last section is used to calculate the magnitude of the reflection coefficient versus frequency for a grating with sinusoidal corrugation having groove depth of 200 μm in a 5mm thick aluminum plate. The effect of grating length on the amplitude of the reflected signal is shown in Fig.2 where it is seen that reflection increases with increasing grating length. The effect of variable groove depth for a fixed grating length gives the same result as that of variable grating length and fixed groove depth for the same groove depth-grating length product.Thus, a grating that is 10 wavelengths long with grooves that are 200 μm deep is equivalent to a grating 20 wavelengths long with grooves that are 100 μm deep. These theoretical results are in good agreement with those of Bavencoffe *et al*. [12] obtained by using the finite element method. The analytical solution will be compared with the results of an experiment as explained in the next section.

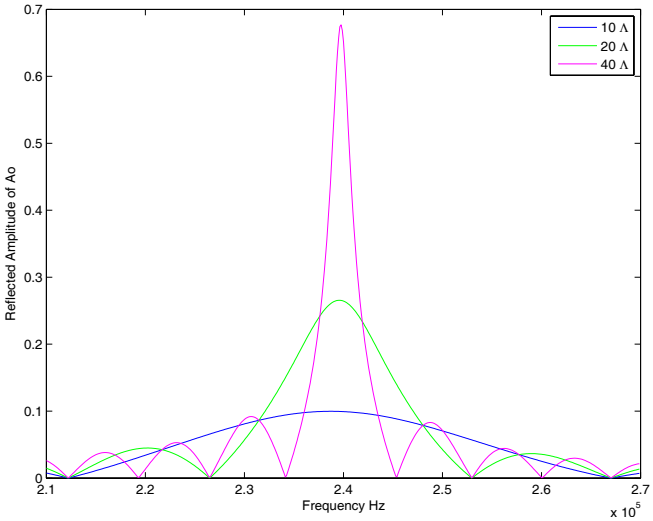

Figure 2: Spectral evolution of reflected antisymmetric mode from analytical solution

6 Experimental results

In the experiment, a 3 mm thick aluminum plate was engraved with a periodic triangular grating having 30 grooves 120 μm deep with a 4.2 mm corrugation wavelength. A S_0 Lamb wave is generated on the flat part of the sample by applying a 10 period electrical tone burst to a contact emitter transducer. The frequency band pass of the emitter transducer is sufficiently large to cover a large frequency range around the first hybridization gap. Normal surface displacements were measured versus time at different positions in the direction of propagation of the incident and reflected waves by means of a laser velocimeter *Polytec*®.Fast Fourier transforms applied to these measurements allow a representation of the amplitude of the reflected wave versus frequency. Figure 4 depicts the power reflection coefficient that is the ratio of the x-components of the reflected and incident energy flux vectors [14]. The results of the experiment were obtained from four different measurements performed with the four different frequencies of the exciting tone burst shown in the inset of Fig.3. The overlapping of the resulting curves demonstrates the robustness of the experimental set-up as well as the signal processing used. The analytical solution for the sample used in the experiment is shown in Fig.5 where the amplitude of the first harmonic of a triangular wave was used in the computation. The agreement with the experimental curve is obvious in shape with two differences in peak amplitude and frequency shift of the maximum response. The frequency shift can be explained by the fact that the depth and width of the machined grooves can slightly vary from the theoretical ones. The theoretically calculated energy of the signal is obviously greater than that of the signal in the experiment. This is expected because the theory did not account for the observed experimental loss due to beam spreading in the plate.

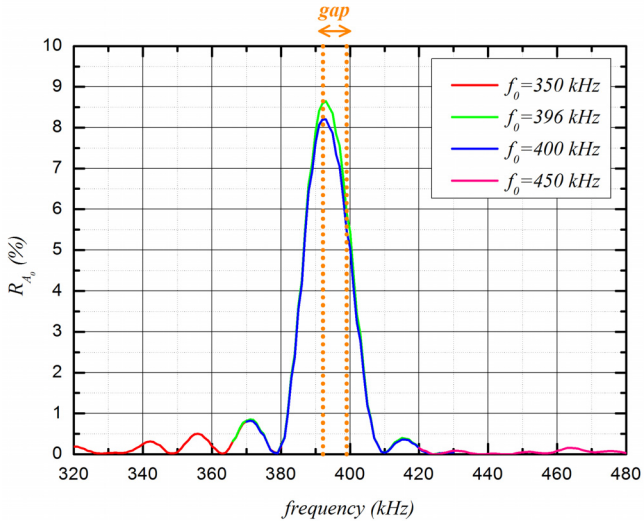

Figure 3: Energy conversion coefficient of the S_0 incident wave on the grating from experiment.

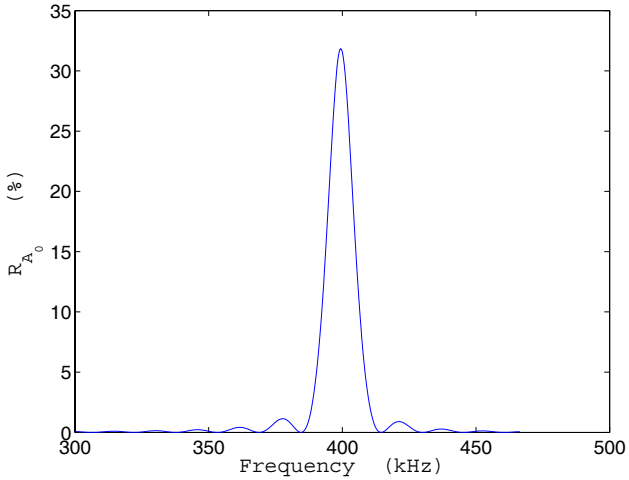

Figure 4: Energy conversion coefficient of the S_0 incident wave on the grating from analytical solution for the sample used in the experiment.

7 Conclusions

An analytical model for the problem of mode conversion in periodically corrugated elastic plates is developed via the perturbation method of multiple scales leading to a closed form expression for the amplitudes of the interacting symmetric S_0 and antisymmetric A_0 modes. The theoretical results are in very good agreement with simulation using finite elements and showed good qualitative agreement with experiment.

8 Appendix: Abbreviations

Given $\gamma_s = \frac{2\alpha_l k_{sx} \sin\alpha_l}{(\alpha_s^2 - k_{sx}^2)\sin\alpha_s}$ and $\gamma_A = \frac{2\beta_l k_{Ax} cos\beta_l}{(\beta_s^2 - k_{Ax}^2) cos\beta_s}$, then

$$\zeta_{11} = 2\mu\alpha_s k_{sx} cos\alpha_s \, P_1 - (k_{sx}^2 - \alpha_s^2) cos\alpha_l \, P_2$$

$$\zeta_{12} = -\left[2\alpha_s k_{sx} cos\alpha_l \, cos\alpha_s\right] Q_{11} + \left[(k_{sx}^2 - \alpha_s^2) cos\alpha_l \, sin\alpha_s\right] Q_{12}$$

$$\zeta_{21} = 2k_{Ax}\beta_s \, sin\beta_l \, sin\beta_s \, Q_{21} + (k_{Ax}^2 - \beta_s^2) cos\beta_s \, sin\beta_l \, Q_{22}$$

$$\zeta_{22} = -2\mu k_{Ax}\beta_s \, sin\beta_s \, P_3 + (k_{Ax}^2 - \beta_s^2) \, sin\beta_l \, P_4$$

where

$$P_1 = 2k_{sx}^2 \left(2 + \frac{sin2\alpha_l}{\alpha_l}\right) - 2\alpha_l \, sin2\alpha_l - 8\gamma_s k_{sx} \, sin\alpha_s \, cos\alpha_l$$

$$P_2 = -2\mu \, k_{sx}^2 \gamma_s \left(2 - \frac{sin2\alpha_s}{\alpha_s}\right) -2\mu \, sin\alpha_s \, (4k_{sx} \, sin\alpha_s \, cos\alpha_l - \alpha_s \gamma_s \, sin2\alpha_s)$$

$$P_3 = 2k_{Ax}^2 \left(2 - \frac{sin2\beta_l}{\beta_l}\right) + 2 \, sin\beta_l \, (\beta_l \, cos\beta_l + 2\gamma_A k_{Ax} \, cos\beta_s)$$

$$P_4 = -2\mu k_{Ax}^2 \gamma_A \, (2 + \frac{sin2\beta_s}{\beta_s}) -4\mu cos\beta_s \, [2k_{Ax} sin\beta_l - \beta_s \gamma_A \, sin\beta_s]$$

$$Q_{11} = sin\beta_l \left[\mu k_{Ax}(\beta_l^2 + k_{Ax}k_w) + \frac{1}{2}\lambda k_w (\beta_l^2 + k_{Ax}^2)\right] + \frac{1}{2}\mu\beta_s\gamma_A \left[\beta_s^2 - k_{Ax}^2 + 2k_{Ax}k_w\right] sin\beta_s$$

$$Q_{12} = -\mu \left[\beta_l^3 \, cos\beta_l + \gamma_A k_{Ax} \beta_s^2 cos\beta_s\right] - \frac{1}{2}\lambda\beta_l(\beta_l^2 + k_{Ax}^2) cos\beta_l$$

$$Q_{21} = -\left[\frac{1}{2}\lambda k_w(\alpha_l^2 + k_{sx}^2) + \mu k_{sx}(\alpha_l^2 + k_{sx}k_w)\right] cos\alpha_l + \mu\alpha_s\gamma_s \left[\frac{1}{2}(\alpha_s^2 - k_{sx}^2) + k_{sx}k_w\right] cos\alpha_s$$

$$Q_{22} = \frac{1}{2}\lambda\alpha_l(\alpha_l^2 + k_{sx}^2) \, sin\alpha_l + \mu(\alpha_l^3 \, sin\alpha_l + k_{sx}\alpha_s^2\gamma_s \, sin\alpha_s)$$

References

[1] O. Lobkis, D. Chimenti, "Elastic guided waves in plates with surface roughness. I. Model Calculation", *J. Acoust. Soc. Am.* **102** (1), 143-149 (1997)

[2] O. Lobkis, D. Chimenti, "Elastic guided waves in plates with surface roughness. II. Experiments", *J. Acoust. Soc. Am.* **102**(1), 150-159 (1997)

[3] A. El-Bahrawy, "'Stopbands and passbands for symmetric Rayleigh-Lamb modes in a plate with corrugated surfaces"' *J. Sound Vib.* **170**(2), 145-160 (1994)

[4] S. Banerjee, T. Kundu, "Symmetric and anti-symmetric Rayleigh-Lamb modes in sinusoidally corrugated waveguides: An analytical approach", *Int. J. Solids Struct.* **43**, 6551-6567 (2006)

[5] P. Waterman, "Scattering by periodic surfaces", *J. Acoust. Soc. Am.* **57**(4), 791-802 (1975)

[6] T. Valier-Brasier, C. Potel, M. Bruneau, P. Catignol, "'Analytical approach of Lamb waves coupling in rough isotropic plates"', *J. Appl. Phys.*, **109**(6), 064902 (2011)

[7] A. Nayfeh, "Sound waves in two-dimensional ducts with sinusoidal walls", *J. Acoust. Soc. Am.* **56**(3), 768-770 (1974)

[8] O. Asfar, A. Nayfeh, "The application of the method of multiple scales to wave propagation in periodic structures", *SIAM Review* **25**(11), 455-480 (1983)

[9] O. Asfar, M. Bataineh, M. Hawwa, "Ultrasonic waveguide with square wave surface grating", *IEEE Trans. Ultrasonics, Ferroelectrics and Frequency Control* **57**(8), 1797-1803 (2010)

[10] D. Leduc, A.-C. Hladky-Hennion, B. Morvan, J.-L. Izbicki, P. Pareige, "Propagation of Lamb waves in a plate with a periodic grating: Interpretation by phonon", *J. Acoust. Soc. Am.* **118**(4), 2234-2239 (2005)

[11] B. Morvan, A.-C. Hladky-Hennion, D. Leduc, J.-L. Izbicki, "'Ultrasonic guided waves on a periodical grating: Coupled modes in the first Brillouin zone", *J. Appl. Phys.* **101**(11),114906-114906-7 (2007)

[12] M. Bavencoffe, A.-C. Hladky-Hennion, B. Morvan, J.-L. Izbicki, " Attenuation of Lamb waves in the vicinity of a forbidden band in a phononic crystal"', *IEEE Trans. Ultrasonics, Ferroelectrics and Frequency Control* **56**(9), 1960-1967 (2009)

[13] D. Royer, E. Dieulesaint, *Elastic Waves in Solids*, New York, NY: Springer (2000)

[14] B. Morvan, N. Wilkie-Chancellier, H. Duflo, A. Tinel, J. Duclos "Lamb wave reflection at the free edge of a plate", *J. Acoust. Soc. Am.* **113**(3), 1417-1425 (2003)